UNCERTAINTY QUANTIFICATION OF MICROCLIMATE VARIABLES IN BUILDING ENERGY SIMULATION

Yuming Sun[1], Yeonsook Heo[1], Huizhi Xie[2], Matthias Tan[2], Jeff Wu[2], Godfried Augenbroe[1]
College of Architecture, Georgia Institute of Technology, Atlanta, USA
School of Industrial and Systems Engineering, Georgia Institute of Technology, Atlanta, USA

ABSTRACT

Since the last decade, it has seen a surge in the need of uncertainty analysis for building energy assessment, but it is often overlooked that the vital part of uncertainty analysis is the determination of uncertainty in model parameters. Significant discrepancy in microclimate state variables has been observed between the predictions and the true climates around the building. This paper quantifies the uncertainty stemming from different sources in the major microclimate variables: local temperature, wind pressure, and solar irradiation, which are used in the statement of the boundary conditions in building energy simulation tools. Although our analysis does not single out a specific simulation tool, we will explore EnergyPlus preprocessing calculations for microclimate as the test case to implement our uncertainty quantification approach.

INTRODUCTION

There is an increasing need to perform uncertainty analyses (UA) of building performance. Such analysis is for instance warranted to support risk-conscious decision making in building design and retrofit when decision are driven by return on investment expectations, or when energy savings guarantees are part of the performance contract. In current practice a building simulation is routinely performed with best guesses to input parameters the true value of which cannot be known exactly. Obviously, these guesses directly affect the accuracy and reliability of the outcomes. Although best guesses can (in our most optimistic beliefs) lead to simulation outputs whose mean roughly corresponds to the mean of the true outcomes, the true variability of all possible outcomes is not discovered unless a full uncertainty analysis is conducted. Instead of taking best guesses, uncertainty analysis considers input parameters as uncertain and propagates the uncertainty through the model by sampling from the distribution of these input parameters. A general procedure of uncertainty analysis can be found in the reference (de Wit and Augenbroe 2002).

A building simulation tool is a collection of many program modules that work together to calculate final outcomes. Each module performs a specific function. It is noteworthy that uncertainty existing in any module has many origins: physical parameter uncertainty, module inadequacy (i.e. modeling errors, also referred to as "code errors"), observation errors, and unknown deterioration effects. Physical parameter uncertainty reflects the variation of parameters under specified conditions. Even if physical parameter uncertainty is ruled out, i.e. all required input parameters can be assigned the true values, the prediction will not equal to the true value of the process as there will always be a certain level of model inadequacy. Observation error accounts for the discrepancy between measurements and true value, which means that the true value is merely a fiction that cannot be measured accurately, but we won't address that part in this paper.

In this paper the focus is on the physical uncertainty in micro climate conditions, typically expressed in micro climate variables that enter into the boundary conditions of the building shell. In most building simulation tools these parameters are obtained by a preprocessing step which transforms meteorological station weather data to building microclimate parameters. The following parameters enter into boundary conditions of energy simulation: local wind speed, local temperature, wind pressure, and total solar irradiation (direct and diffuse). Each simulation tool may deploy its own flavor of preprocessing calculation but the differences across the current leading tools are not significant. We will refer to the current pre-processing as the "standard model" in this paper. The standard model implemented in current simulation tools for micro climate conditions is rather crude and its representation of urban surroundings lacks sufficient detail. The UQ in this paper is not limited to specific simulation software, but as EnergyPlus is regarded as a representative high-end simulation application, it is used as starting point for the standard model of the microclimate parameters.

By comparing its results with higher fidelity meso-scale models, we can quantify the uncertainty stemming from module inadequacy as well as insufficient knowledge. The major purpose of this UQ approach is twofold: (1) to propagate the uncertainty through the simulation model of the whole building and quantify uncertainty in an outcome such as total consumed energy; (2) to enable the ranking of all microclimate parameters on their highest impact on a certain outcome, accomplished

through sensitivity analysis. The latter is an important result as it implicitly shows which parts of the standard model may need improvement to increase the fidelity of the simulation tool.

BUILDING MICROCLIMATE

Information about the building microclimate is usually unavailable, thus requiring some form of preprocessing calculation to transform recorded weather data from a nearby meteorological station to microclimate conditions. However, as shown in Figure *1*, the microclimate around the building is affected by various factors such as surrounding vegetation, location of neighboring objects, meso-scale air flow patterns etc. These effects results in the significant discrepancy with meteorological station weather data and actual micro climate conditions.

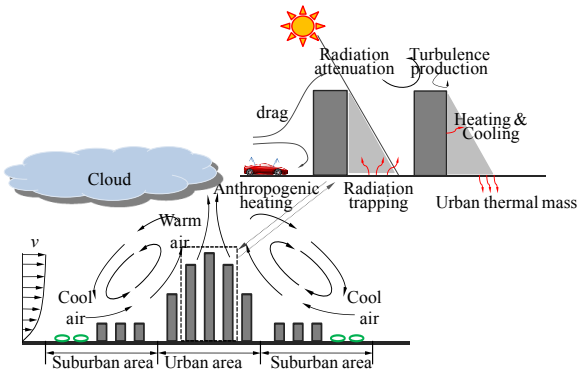

Figure 1 Suburban and urban climate

In order to derive the building microclimate from far away meteorological weather data, the model needs to accurately capture air flow patterns around the building, temperature variations due to urban heat island, the existence of complex urban plumes in major metropolitan regions, and other phenomena. This would require a deep urban representation as well as a computational intensive numerical model. Although these kinds of models have been well developed at different scales, i.e. for regional weather forecasting and urban scale modeling, they have not yet been integrated with the current generation of building simulation tools. This study performs an UQ of standard models such as those adopted by EnergyPlus. The uncertainty in four microclimate state variables are studied in detail: (1) local wind speed, (2) local temperature, (3) wind pressure, and (4) total solar irradiation including direct, diffuse, reflected radiation. The standard model calculates these variables using weather data from a meteo station with partial consideration of the urban surrounding of the building under consideration and the distance between meteo station and the building. It should be noted that the standard model uses some form of urban characterization in the calculation. For instance, the calculation of local wind speed around the building utilizes two coefficients in the transformation of the meteorological weather data to the building's micro climate wind speed variable. Another instance is the calculation of solar irradiation on vertical surfaces which uses a user specified reflectance of ground surfaces to approximate what is typically a combination of many surfaces with different reflectivity.

It is obvious that the standard model for generating the microclimate variables is unreliable and in any case is too crude to investigate the effects of urban surroundings on the local microclimate. So far a rigorous uncertainty analysis of microclimate conditions has not been performed. This is an omission as it is well known that micro climate variables can have significant influence on local temperature, convective heat transfer coefficients, ex- and infiltration, reliance on natural ventilation, and solar heat gains. The motivation for this paper is to conduct a UQ for the micro climate variables, as a preparation towards uncertainty propagation and effect ranking to guide future model improvements. This paper only deals with the first part, the UQ.

UNCERTAINTY QUANTIFICATION

This section shows how meso-scale models are used to quantify uncertainty in current standard microclimate models used for the preprocessing in simulation tools. First we investigate meso-scale models that adequately represent the effects of urban surroundings on microclimate conditions. Then, we conduct pairwise comparisons between meso-scale model outcomes and standard model outcomes, and analyze their differences. Figure 2 shows the UQ process. Both the standard model and higher fidelity meso-scale model need meteorological station weather data and an urban built form representation as input. Wind speed and wind pressure standard models only recognize a crude representation of the urban form specification in the form of a terrain classification defined in the ASHRAE Handbook (i.e., open country, urban and suburban areas, and large city center (ASHRAE, 2005).

This categorical information leaves a lot of variability in the urban form of each category. This variability intrinsically results in uncertainty as the specific built form is not regarded in the standard model. The effect of this variability is examined by generating a set of experimental situations within each terrain classification to explore the effects of all plausible urban contexts. For each experimental situation, we can now calculate the differences between the two model outcomes. Aggregation of all estimates leads to distributions of uncertainty in the two microclimate state variables. There is no standard model for the calculation of local temperature, which means meteorological station data for air temperature is assumed to be the local micro climate variable. In this case, we assume that only a low level urban knowledge about the urban form is available just because most standard models follow this rule. For solar irradiation, we focus on how the standard model (algorithm) distributes solar irradiation on building surfaces by considering

shading, reflection, etc. In general, the standard model in current simulation tools supports specification of building surroundings, which thus reflects a higher level of urban form knowledge.

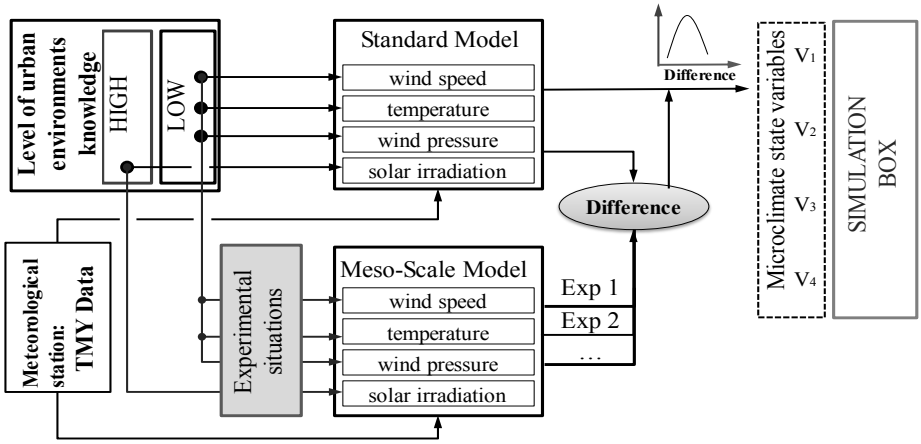

Figure 2 Microclimate uncertainty quantification framework

For direct solar irradiation the standard model calculates sun position and shadow area accurately enough such that the discrepancy between its outcomes and a better meso-scale model is negligible. For the diffuse solar irradiation the standard model employs the well-known Perez model. In ongoing work (not reported here) the uncertainty of the Perez model (Perez, 1987) outcomes are quantified based on experimental data. With regard to solar irradiation, this paper only shows the result for the ground reflected solar irradiation with and without snow presence.

A global dataset of urban form and building properties was developed to study the urban climate (Jackson, Feddema et al. 2010). The dataset includes the urban morphology and physical characteristic of building materials across 33 regions of the world and subdivides urban area into four levels of urban density: tall building district, high, medium and low density urban. This study uses this dataset to consider the variability of urban form.

1. local wind speed

Typically simulation software follows Chapter 16 of ASHRAE Fundamentals (ASHRAE, 2005) to compute local wind speeds in the local terrain. ASHRAE Fundamentals specifies a method that computes local wind speeds at a certain height from the measured wind speed (V_{met}) at the meteorological station with use of a wind reduction factor. The wind reduction factor is derived as a function of measurement height (z), wind exponent (α), and boundary layer thickness (δ) for the site and the meteorological station as expressed in Equation1. ASHRAE Fundamentals provides default values for α and δ for three terrain types. Typically in simulation modeling, users select values of the two parameters based on a site terrain type.

$$V_z = V_{met}\left(\frac{\delta_{met}}{z_{met}}\right)^{\alpha_{met}}\left(\frac{z}{\delta}\right)^{\alpha} \quad (1)$$

For the meso-scale model, we selected part of a Community Land Model (CLM) that computes average local wind speeds in the urban context (Oleson, 2008). It approximates urban surroundings, following the urban canopy concept. Figure 3 represents the CLM urban form parameterization scheme; all buildings are identical in terms of their geometry, and they are regularly distributed over the urban grid; the open space between two rows of buildings is defined as a canyon. This approximation enables 3-D complex urban form representation to be transformed into a 2-D layout. CLM parameterizes urban surroundings by the three geometric variables: (1) canyon height (H), (2) canyon ratio (H/W), and (3) building length-to-width ratio (B_L/B_W). The urban parameterization scheme is used to capture all variability in heat transfer in the urban context such as drag effects and radiation trapping.

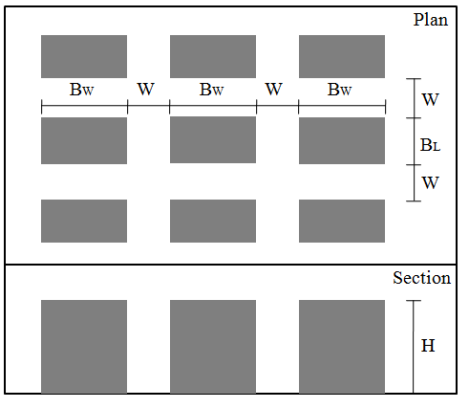

Figure 3 Urban parameterization scheme in the Community Land Model

As CLM outcomes, we obtain average local wind speeds in the canyon areas surrounding a building at a given measurement height. That is, CLM does not capture variation of local wind speeds along building surfaces at a given measurement height. As a result, the difference between the ASHRAE model and CLM outcomes only quantifies uncertainties in average local wind speeds (i.e. averaged along the horizontal perimeter of the building shape at a given height). Hence, in order to quantify all sources of

uncertainty in local wind speeds for different positions on the building facade, we will introduce an additional term that explains potential deviations from the average speed quantified by our analysis.

First experimental situations were generated for a set of urban surroundings, separately for the three terrain types. We set up experimental designs in terms of the three urban geometric parameters based on the global dataset (Jackson, 2010) introduced above. Since the dataset shows high correlations between canyon height and canyon ratio in cities and urban terrains, we used actual cases from the dataset in the design rather than randomly generated samples. The rest is considered independent. From the actual cases and the range of independent parameter values, we used Latin Hypercube Sampling (Wyss, 1998) to obtain 260, 990, and 50 situations for cities, urban, and open country respectively. In the same manner, we also generated 20 situations for meteo station surroundings.

Table 1 Setup for Experimental Design

	H		H/W		B_L/B_W	
	min	max	min	max	min	max
Country	3	3	0	0.3	0.25	1.00
Urban	99 cases from the dataset				0.25	1.00
Cities	26 cases from the dataset				0.25	1.00

The purpose of the UQ framework is to model the difference between the output from the ASHRAE model and that from CLM. In this case a log scale is used. Through the difference modeling, we quantify the inadequacy of the ASHRAE model and uncertainty induced by not accurately specifying urban surroundings. We generate different situations in each terrain, and use statistical techniques to model the difference for each situation. Due to the length limit, we focus on the terrain of city in the following presentation. Through some exploratory analysis, the following statistical model is proposed to model the difference as a function of the measured height z.

$$\text{Diff} = \begin{cases} \beta_{01} + \beta_{11} z + \varepsilon & \varepsilon \sim N(0, \sigma^2) \quad z \le \tau \\ \beta_{02} + \beta_{12} z + \varepsilon & \varepsilon \sim N(0, \sigma^2) \quad z > \tau \end{cases} \quad (2)$$

For each situation in the terrain of a city, we estimate the unknown parameters β_{01}, β_{11}, β_{02}, β_{12}, τ and σ^2 using maximum likelihood estimation(Mendenhall, Beaver, and Beaver 2008). This results in a point estimate for these parameters for each situation. The histograms of the estimates of these parameters, induced by the different situations, are presented in Figure 4. From a statistical point of view, the sample size in each situation is large enough. So the shape of histograms should be robust to the random errors from the meteo station surroundings. But keep in mind the shape of the histograms depends on the experimental situations we have used.

The R^2 for all the situations is above 0.95. Most situations enjoy a R^2 above 0.99, indicating the goodness-of-fit of the piecewise linear model employed here. Given the fitted statistical model, for any value of measured height z, a distribution of the difference between the outputs of the ASHRAE model and the meso-scale model results is derived. Note that the variation in the distribution represents the variation among different situations as well as the variation among the surroundings of the meteo station in each situation. By adding the distribution of differences for each measurement height to the outcomes of the ASHRAE standard model, the uncertainty in the local wind speed state variable is quantified.

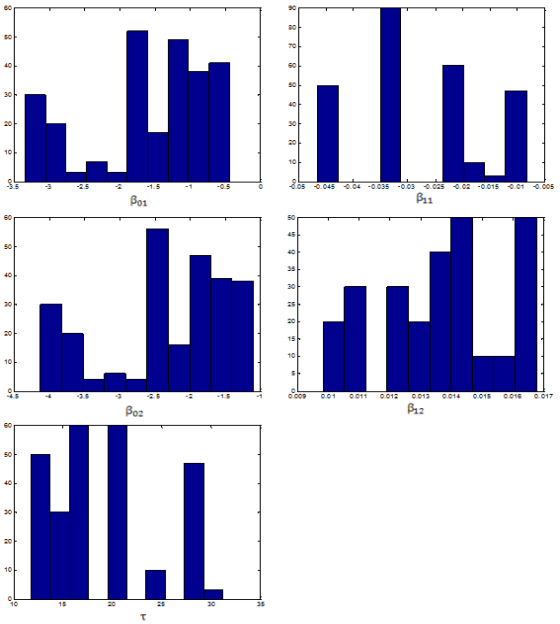

Figure 4 Histograms of unknown parameters

2. Urban heat island effect

Temperature discrepancy between the location of the meteo station and the building site caused by urban heat island (UHI) effect is not taken into account by the standard model in current simulation tools. In this section, it is shown how UQ was performed based on the town energy budget (TEB) model (Masson 2000). The TEB model simulates heat and moisture exchange through walls, roofs and roads by numerically solving energy balance equations. The model has been shown to be capable of accurtely predicting energy fluxes, canyon air temperatures, and surface temperatures (Masson, Grimmond et al. 2002). To compute UHI intensity, we first applied this model under urban conditions with surfaces consisting of town and nature components for the urban canyon air temperature prediction. Then, a second run was performed under rural conditions with grassland covering the entire surface to compute temperature difference with the first run. The forcing atmospheric weather conditions were derived from TMY weather data through a simple calculation. This led to the required weather parameters for the model, which are: short-wave (w_1) and long-wave (w_2) solar radiation, air temperature (w_3), wind speed (w_4), pressure (w_5), specific humidity (w_6).

UQ was performed at an hourly basis in order to be able to verify the diurnal characteristic of the heat island phenomenon. We used whole-year TMY2 data of 16 DOE benchmark cities (Paul Torcellini, 2008) in 16 climate zones of the US to analyze the effect of climate. As an example, this section shows results for Atlanta, city terrain type. The urban geometry was shown to be the most influential factor on UHI intensity. Thus, we consider all urban geometry related parameters as uncertain in the TEB model; *Table 2* lists the min and max value of urban geometric parameters. We don't consider UHI effect for the building situated in open country.

Table 2 Geometric parameters of TEB model

Terrain		α^*_{roof}	α^*_{perv}	H(m)	H:W
Cities	min	40%	12.5%	60	W=25m
	max	85%	71.4%	200	
Urban	min	5%	10%	99 Cases	
	max	90%	80%		

α^*_{roof} :Area fraction occupied by roof; α^*_{perv} : Area fraction of pervious road to total road area

Roof, road and wall material properties are set according to the Vancouver case introduced in Masson's paper (Masson, Grimmond et al. 2002), because these materials are more likely to represent the thermal properties of the US cities (Oleson, Bonan et al. 2008).

We develop statistical models for predicting the time series of UHI intensity, ΔT , for various scenarios in Atlanta. For simplification, we define the notations here. Hourly weather data comprises of six variables $\boldsymbol{w} = (w_1, \dots, w_6)^T$ mentioned above over the period of one year. Three physical parameters $\boldsymbol{z} = (z_1, z_2, z_3)^T$ (z_1: building height, z_2: area fraction occupied by roof, z_3: area fraction of pervious road area to total road area) that characterize a scenario. It was found that for any fixed scenario, the relationship between ΔT and $\boldsymbol{w} = (w_1, \dots, w_6)^T$ can be modeled well by the regression equation:

$$\Delta T = \beta_0 + \sum_{i=1}^{6} \beta_i w_i + \beta_7 T_r, \qquad (3)$$

Where, T_r is the mesoscale prediction of the rural temperature. We estimate $\boldsymbol{\beta} = (\beta_0, \beta_1, \dots, \beta_7)^T$ by regressing the hourly time series of ΔT versus the hourly time series of $(\boldsymbol{w}, T_r)$. The value of R^2 is generally found to be between 75% and 80%. We study the effect of $\boldsymbol{z}$ on $\boldsymbol{\beta}$ and build statistical models for predicting $\boldsymbol{\beta}$ based on $\boldsymbol{z}$. The experiment region is taken as $[60,200] \times [0.40,0.85] \times [0.125,0.714]$. In the following analysis, we shall work with the variable $\boldsymbol{x} = (x_1, x_2, x_3)^T$, which is $\boldsymbol{z}$ rescaled so that the experiment region is $[0,1]^3$. A 24-run maximin Latin Hypercube design (LHD) is employed for the experiment. Data from the experiment is used to construct the Gaussian process (GP) emulators (Santner et al., 2003; Sacks et al., 1989) $\hat{\beta}_j(\boldsymbol{x})$ for $j = 0,1, \dots,7$. Since T_r is unknown and depends on $\boldsymbol{w} = (w_1, \dots, w_6)^T$, we would also need to build an interpolator (e.g., inverse distance interpolator (IDI) (Joseph and Kang, 2011)) $\hat{T}_r(\boldsymbol{w})$ to predict T_r if we want to predict ΔT for a different set of weather data.

Note that a LHD is a space-filling design used in computer experiments for the purpose of fitting highly nonlinear interpolators such as a GP emulator. A GP emulator is a statistical interpolator obtained by modeling the unknown function f as a Gaussian process, i.e. $f \sim GP(\mu(\cdot), cov(\cdot,\cdot))$, where $\mu(\cdot)$ is the mean function and $cov(\cdot,\cdot)$ is the covariance function. The emulator value at $\boldsymbol{x}$, i.e., $\hat{f}(\boldsymbol{x})$ is the conditional expectation of $f(\boldsymbol{x})$ given the data $(f(\boldsymbol{x}_1), \dots, f(\boldsymbol{x}_n))$. An important property of the GP emulator is that $\hat{f}(\boldsymbol{x}_j) = f(\boldsymbol{x}_j)$ (this justifies its use for interpolating deterministic output). An IDI is a simpler interpolator. It is more suitable for interpolating large data sets (such as the data for T_r) due to its low computational requirements.

It was found for all 24 time series of temperature difference produced by the experiment have similar patterns and this cyclical variation that repeats on a daily basis tended to be dominant compared to the month-to-month difference. Maximum UHI intensity appears during nighttime and deceases to its minimum around the middle of a day (*Figure* 5).

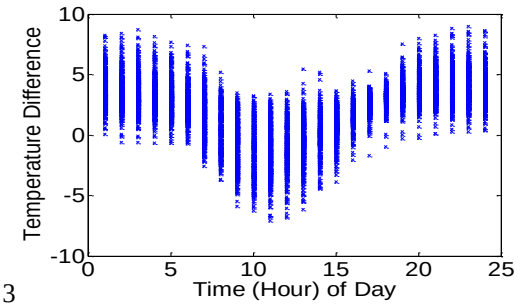

3

Figure 5 Plot of temperature difference versus hour of day for One Scenario (One Year's Data)

For all of the 24 runs, the weather variable w_5 has a small regression coefficient β_5 and in many of the runs, it is insignificant at the 5% level. All other coefficients are large and distinguishable from zero in all runs (except for an insignificant β_2 for in of the runs). The coefficients $\beta_1, \beta_3, \beta_4, \beta_6$ are positive in all experiment runs whereas β_2, β_7 are negative in all runs. Each of the coefficients except β_5 exhibit a clear linear trend when plotted against x_1. On the other hand, the plot of β_5 against x_1 suggests that the relationship between β_5 and x_1 is governed by a step function.

We evaluate the predictive performance of the GP emulators $\hat{\beta}_j(\boldsymbol{x})$. Four confirmation runs are performed at four different $\boldsymbol{x}$'s distinct from the design points. In

, the actual values of the β_j's for one of these runs are compared with the predictions, i.e., the $\hat{\beta}_j(\boldsymbol{x})$'s. Also shown in the table are 95% prediction intervals ($[LCL, UCL]$). It is seen that the predictions are very

close to the actual values, which are all within the prediction intervals. A plot (not shown) of the predicted and actual temperature difference for the confirmation run also show that predictions are reasonably close to the meso-scale model output.

Table 3 Validation of Statistical Model

	$\boldsymbol{x} = (1,0,0.0085)$			
	LCL	UCL	Prediction	Actual
β_0	15.952	16.8	16.376	16.04
β_1	-0.00019	3.78E-05	-7.7E-05	8.4E-06
β_2	-0.00716	-0.00662	-0.00689	-0.00668
β_3	0.88714	0.92212	0.90463	0.91521
β_4	0.025534	0.028776	0.027155	0.026392
β_5	-0.00013	-0.00012	-0.00012	-0.00012
β_6	61.353	65.393	63.373	62.405
β_7	-0.9183	-0.88579	-0.90205	-0.91257

3. Wind pressure

The standard model in most simulation software follows Chapter 16 of ASHRAE Fundamentals (ASHRAE, 2005) to compute wind pressures on a building. Wind pressure on a building surface depends on ambient air density (ρ), local wind speed (V_z), and wind surface pressure coefficients (C_p) as defined in Equation 4. ASHRAE Fundamentals describes empirically driven models that generate surface-averaged pressure coefficients for low-rise buildings (Swami and Chandra, 1987) and high-rise buildings (Akins, 1979). All models are defined as a function of the wind incident angle and the ratio of the width of the wall under consideration to that of the adjacent wall.

Equation 5 indicates the Swami and Chandra model as a function of wind incident angle (θ) and the natural log of the ratio (G). All models are based on wind-tunnel experiments for a stand-alone building without accounting for the interfering effects of neighboring buildings.

$$P_w = C_p \rho \frac{{V_z}^2}{2} \tag{4}$$

$$C_p = 0.6 \ln \begin{pmatrix} 1.248 - 0.703 \sin\left(\frac{\theta}{2}\right) - 1.175 \sin^2(\theta) \\ + 0.131 \sin^2(2\alpha G) + 0.769 \cos\left(\frac{\theta}{2}\right) \\ + 0.07 G^2 \sin^2\left(\frac{\theta}{2}\right) + 0.717 \cos^2\left(\frac{\theta}{2}\right) \end{pmatrix} \tag{5}$$

For the higher fidelity meso-scale model, we employed the TNO Cp generator that calculates wind surface pressure coefficients in the urban context. The Cp generator is a parametric model developed based on experimental data that calculates coefficient values based on wind direction and building dimensions and corrects coefficient values, taking the surrounding terrain into account. (Knoll, 1995). The Cp generator requires information about full geometries and terrain roughness for adjacent obstacles and for distant obstacles respectively. As outcomes, we obtain surface-averaged coefficient values for each wall for each wind direction. We follow the urban parameterization scheme in the Climate Land Model to represent surroundings in which a building under consideration may be situated: this leads to the selection of eight identical buildings surrounding the building under consideration. Configuration of the buildings and their spatial relationships are parameterized by the four variables: canyon height (H), canyon ratio (H/W), building height-to-length ratio (H/B_L), and building width-to-length ratio (B_W/B_L). With the four variables and terrain roughness factor, we generated 81 situations for a range of various urban situations based on the ranges and cases shown in Table 4. Due to the time-consuming simulation setup, we use three distinct values of B_W/B_L in the simulation experiments, i.e., $1,2,4$. We model the difference as a function of incident angle separately for each B_W/B_L value because of the scarcity of B_W/B_L samples. The following statistical model is utilized.

$$\text{Diff} = \begin{cases} f_1(\theta) + \varepsilon_1 & \varepsilon_1 \sim N(0, \sigma_1^2) \quad \text{for } \frac{B_W}{B_L} = 1 \\ f_2(\theta) + \varepsilon_2 & \varepsilon_2 \sim N(0, \sigma_2^2) \quad \text{for } \frac{B_W}{B_L} = 2 \\ f_3(\theta) + \varepsilon_3 & \varepsilon_3 \sim N(0, \sigma_3^2) \quad \text{for } \frac{B_W}{B_L} = 4 \end{cases} \tag{6}$$

The question is how to estimate the $f_i(\theta)$'s. We tried smoothing spline models, local polynomial regression models, stochastic kriging models for the estimation of $f_i(\theta)$'s. The results all look similar. The common message is that a large portion of the variation of the pressure coefficient cannot be explained by the incident angle. In order to quantify the effect of B_W/B_L, we propose to fit a global parametric model for the $f_i(\theta)$'s for each B_W/B_L. By trial and error, we found a fourth-order polynomial regression model is adequate for all the three cases in the sense that the residual behavior of the polynomial regression models is similar to the aforementioned nonparametric models. The polynomial regression model for each case of B_W/B_L is specified as Equation 7.

$$f_i(\theta) = \beta_{0i} + \beta_{1i}\theta + \beta_{2i}\theta^2 + \beta_{3i}\theta^3 + \beta_{4i}\theta^4 \tag{7}$$

where $i = 1,2,3$.

The scatter plots of the difference against incident angle as well as the fitted polynomial regression models are shown in Figure 6.

Table 4 Setup for Experimental Design

	H		H/W		H/B_L		B_W/B_L		Roughness	
	min	max	min	max	min	max	min	max	min	max
Low-rise Building	99 cases from the dataset				1	3	1	4	0.03	7.00

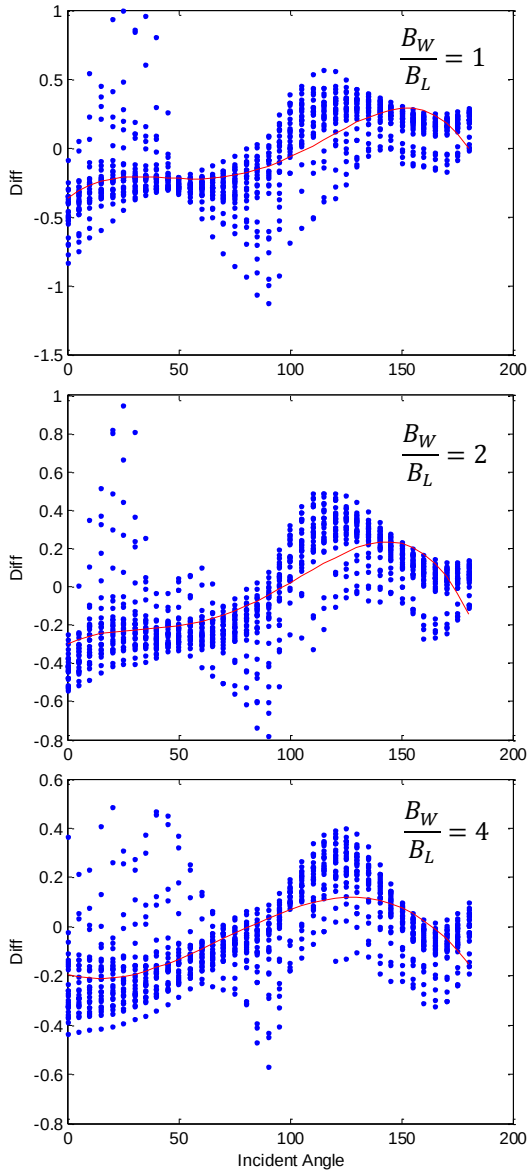

Figure 6 Scatter plots and regression models

Statistical hypothesis testing proved that B_W/B_L has a significant effect on the coefficients $\beta's$ as well as the variance terms $\sigma's$. Hence, we propose to use a linear interpolator to get the coefficients $\beta's$ and the variances term σ for those values of B_W/B_L not included in this analysis. As a result, for any value of B_W/B_L, we can obtain a fourth order polynomial regression model describing the relationship between difference and incident angle. Based on the model, we can issue a distribution of differences between the Swami and Chandra model outcomes and the TNO Cp generator outcomes for any value of incident angle and B_W/B_L. Note that the variation of the distribution is induced by the different urban situations in which a low-rise building case may be located.

4. Solar irradiation

4.1 Ground reflectance

A monthly reflectance of 0.2 is embedded in the calculation engine as default value and is commonly used in practice. In the meso-scale model, ground reflectance considers the road composition of impervious and pervious, calculated by the following equation:

$$\rho_{ground} = \rho_{prvd} f_{prvd} + \rho_{imprvd}(1 - f_{prvd})$$

Where, ρ_{prvd} , ρ_{imprvd}: pervious and impervious road solar reflectance; f_{prvd} , f_{imprvd} : pervious and impervious road area fraction.

The range of each parameter comes from the global dataset and references (Ahrens 2007) (Clarke, Cockroft et al. 2002) and summarized in Table 5.

Table 5 List of parameters and ranges for the generation of experimental situations

Parameters	Cities		Urban/ Suburban		Open Country	
	Min	Max	Min	Max	Min	Max
f_{prvd}	5%	25%	5%	90%	90%	1
ρ_{imprvd}	0.072	0.44	0.072	0.44	0.072	0.44
ρ_{prvd}	0.05	0.4	0.05	0.4	0.05	0.4

The uncertainty in each of the parameters is modeled with independent uniform distributions. For each terrain type, the probability density function (pdf) of ρ_{ground} is estimated by generating a Monte Carlo sample and utilizing this sample to construct a Kernel density estimator. Figure 8 shows the estimated pdf for city terrain. The distribution is centered at around 0.25, and it has a range from about 0.05 to 0.45.

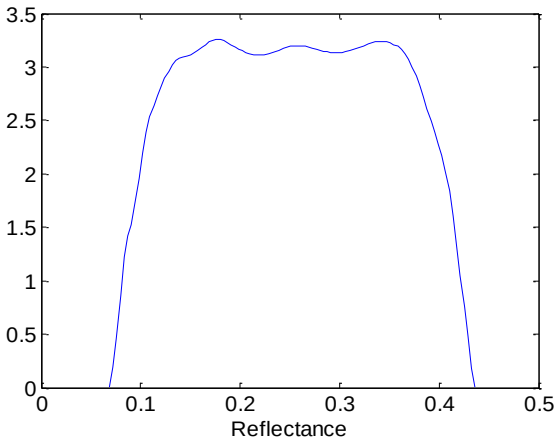

Figure 7 City Terrain PDF Ground Reflectance

4.2 Ground reflectance in the presence of snow

As ground reflectance increases dramatically in the presence of snow, it can vary from 0.75 to 0.95 for fresh snow cover and 0.4 to 0.7 for old snow cover, (T.Muneer 2004) and detailed snow information is not available in the weather data, as a result, it is very difficult to capture the overall snow effect on ground reflectance by a yearly constant value. For urban

area, Hunn and Calaffell's research (Hunn and Calafell 1977) concluded that no characteristic ground reflectance in winter could be specified and they suggested values ranging from 0.16 to 0.49. For the rural area, they suggested ground reflectance of 0.6 to 0.7 for most rural landscape where a large snow cover is visible without obstruction. We will use their findings for further uncertainty analysis.

SUMMARY AND CONCLUSIONS

This paper starts from the recognition that the accuracy of the current generation of simulation tools is affected by many sources of uncertainty. We have focused on one particular set of input variables, i.e. the ones that appear in the micro climate boundary conditions. A UQ framework was introduced, which systematically compares the microclimate state variables computed by the standard model, embedded in current simulation models, with those computed with a higher fidelity meso scale model that also takes more detailed specifications of urban form into account. The approach was applied to five major micro climate state variables. The UQ results were obtained with a variety of statistical techniques. Not surprisingly, given the simplicity of the current standard micro climate models, the uncertainty in using these models has significant magnitude. The resulting expressions will now be used for the ensuing propagation of uncertainty through building simulation models. At that point the effect of the uncertainty in micro climate variables on building energy outcomes will be quantified and recommendations will be generated.

ACKNOWLEDGEMENTS

This study was fully funded by the NSF-EFRI SEED grant: "Risk-conscious Design and Retrofit of Buildings for Low Energy" awarded to the Georgia Institute of Technology.

REFERENCES

Ahrens, C. D. (2007). Meteorology today : an introduction to weather, climate, and the environment. Belmont, Calif., Thomson/Brooks/Cole.

Akins, R. E., Peterka, J. A., and Cermak, J. E. (1979). Averaged pressure coefficients for rectangular buildings. Wind Engineering: Proceedings of the Fifth International Conference, 7:369-380.

ASHRAE. (2005). ASHRAE Handbook Fundamentals. American Society of Heating, Refrigerating and Air-conditioning Engineers. Atlanta, GA.

Clarke, J. A., J. Cockroft, et al. (2002). "Simulation-assisted control in building energy management systems." Energy and Buildings **34**(9): 933-940.

de Wit, S. and G. Augenbroe (2002). "Analysis of uncertainty in building design evaluations and its implications." Energy and Buildings **34**(9): 951-958.

Hunn, B. D. and D. O. Calafell (1977). "Determination of Average Ground Reflectivity for Solar Collectors." Solar Energy **19**(1): 87-89.

Jackson, T. L., J. J. Feddema, et al. (2010). "Parameterization of Urban Characteristics for Global Climate Modeling." Annals of the Association of American Geographers **100**(4): 848-865.

Joseph, V.R. and Kang, L. (2011) "Regression-Based inverse Distance Weighting with Applications to Computer Experiments." Technometrics, to appear.

Knoll, B., Phaff, J. C., and de Gids, W. F. (1995). Pressure simulation program. Proceedings of the conference on implementing the results of ventilation research, AIVC.

Masson, V. (2000). "A Physically-Based Scheme For The Urban Energy Budget In Atmospheric Models." Boundary-Layer Meteorology **94**(3): 357-397.

Masson, V., C. S. B. Grimmond, et al. (2002). "Evaluation of the Town Energy Balance (TEB) scheme with direct measurements from dry districts in two cities." Journal of Applied Meteorology **41**(10): 1011-1026.

Mendenhall, W., Beaver, J. R., et al. (2008). Introduction to probability and statistics, Duxbury press

Oleson, K. W., G. B. Bonan, et al. (2008). "An Urban Parameterization for a Global Climate Model. Part II: Sensitivity to Input Parameters and the Simulated Urban Heat Island in Offline Simulations." Journal of Applied Meteorology & Climatology **47**(4): 1061-1076.

Perez, R., Seals, R., Ineichen, P., Stewart, R., and Menicucci, D. (1987). A new simplified version of the Perez diffuse irradiance model for tilted surfaces. Solar Eerngy, 39(3):221-231.

Sacks, J., Welch, W.J., Mitchell, T.J., and Wynn, H.P. (1989), "Design and Analysis of Computer Experiments," Statistical Science, 4(4), 409-435.

Swami, M. V., and Chandra, S. (1988). Correlations for pressure distribution on buildings and calculation of natural-ventilation airflow. ASHRAE Transactions, 94:243-266.

T.Muneer, Ed. (2004). Solar radiation and daylight models, ELSEVIER.

Wyss, G., and Jorgensen, K. (1998). A user's guide to LHS: Sandia's Latin Hypercube Sampling Software. Sandia National Laboratories, Albuquerque, NM.